RESEARCH ARTICLE

Editorial Process: Submission:01/13/2025 Acceptance:05/17/2025

Polyherbal Formulation as a Therapeutic Strategy for Lung Cancer: Phytochemical Profiling, Molecular Docking, and Pharmacological Evaluation

Raman Lakshmi Sundaram[1], Thirunavukarasou Anand[2]*, Konda Mani Saravanan[3], Kaliyaperumal Prabhu[4], Abdul Mohamed Yasar[5], Srinivasan Vivek[5], Ashok Chetan[5], Jeyabalan Srikanth[5]*

Abstract

Globally, lung cancer continues to be the primary cause of both cancer incidence and death. The disease is multifaceted, influenced by numerous external factors and the individual's genetic or epigenetic predisposition to its onset and timing. Upon diagnosis, fewer than one-third of patients present with localized disease amenable to curative multimodal therapy; the remainder have metastatic disease. Currently, numerous treatments are ineffective due to resistance to standard medications or the emergence of distant metastases. Plant-derived natural compounds have garnered significant attention in recent years due to their high permeability and low toxicity. *Piper longum, Piper nigrum, Zingiber officinalis, Emblica officinale, Terminalia bellirica, Terminalia chebula, Drynaria quercifolia, Phyllanthus amarus*, and *Eclipta prostrata* are traditional Indian herbs with diverse pharmacological properties. This study assessed the efficacy of active chemicals from the polyherbal formulation on lung cancer target proteins by molecular docking. Preliminary and qualitative phytochemical Antioxidant testing indicated significant pharmacological effects. Moreover, the formulation exhibited modest anti-inflammatory and significant apoptotic action. These findings validate the therapeutic effectiveness of this polyherbal mixture for cancer treatment. Nonetheless, it is imperative to perform further preclinical research to elucidate the mechanisms of action of the molecule, as well as its pharmacodynamic and pharmacokinetic features.

Keywords: Lung Neoplasms- Phytotherapy- Molecular Docking Simulation- Antioxidants

Asian Pac J Cancer Prev, **26 (5)**, 1841-1852

Introduction

Lung cancer is the predominant cancer type responsible for mortality in both the United States and worldwide [1]. Despite recent advancements in the early identification and treatment of cancer, lung cancer continues to provide a significant challenge due to its high mortality rate and the limited effectiveness of traditional therapies for localized, advanced, or metastatic malignancies [2]. The National Lung Screening Trial (NLST) has shown that early identification with annual low-dose helical computed tomography scans could decrease lung cancer mortality by 20% compared to chest radiography in high-risk adults [3]. Nevertheless, early detection alone cannot address all issues related to current therapeutic methods, typically marked by the emergence of resistance and significant adverse consequences [4]. Consequently, it is essential to devise novel therapeutic strategies to improve the prognosis of people afflicted with this illness [5–7].

As a result, plant-based therapies have garnered significant attention due to their potential to provide safe and effective treatments in contrast to conventional medicine [8]. Herbal formulations in Ayurveda, an ancient medical system, focus not only on treatment but also on preventing relapse, with the explicit objective of restoring health [9]. Polyherbal formulations involve combining two or more plants and are favored for creating preparations that exhibit enhanced therapeutic efficacy with reduced toxicity [10]. These formulations enhance patient adherence and have a significant pharmacological effect by eliminating the necessity to administer many medications simultaneously [11]. The features above render polyherbal

*[1]Faculty of Pharmacy, Sri Ramachandra Institute of Higher Education and Research, Chennai, Tamil Nadu, India. [2]Faculty of Clinical Research, Sri Ramachandra Institute of Higher Education and Research, Chennai, Tamil Nadu, India. [3]B Aatral Biosciences Private Limited, Bengaluru, Karnataka, India. [4]Department of Anatomy, Sree Balaji Medical College and Hospital, Chennai, Tamil Nadu, India. [5]Department of Pharmacology, Sri Ramachandra Institute of Higher Education and Research, Chennai, Tamil Nadu, India. *For Correspondence: anand.sriic@gmail.com, srikanth.j@sriramachandra.edu.in. Raman LakshmiSundaram and Thirunavukarasou Anand have equal contribution in this study.*

formulations a viable domain for exploring alternative lung cancer treatments [12].

Table 1 lists traditional medicinal plants and formulations, highlighting their common names, botanical names, and composition. It includes formulations like Trikatu [13], composed of equal proportions of long pepper (*Piper longum*), black pepper (*Piper nigrum*), and ginger (*Zingiber officinalis*), and Triphala [14], a mix of amala (*Emblica officinale*), baheda (*Terminalia bellirica*), and chebulic myrobalan (*Terminalia chebula*). The bioactive chemicals in *Zingiber officinale*, known as gingerols, exhibit potent anticancer properties by inducing apoptosis via caspase activation, inhibiting NF-κB signaling, and retarding the proliferation of cancerous tissues and the creation of metastases [15]. Piperine derived from Piper nigrum demonstrates anticancer effects by modulating the PI3K/Akt and MAPK signaling pathways, inducing cell cycle arrest, and enhancing the bioavailability of concurrently delivered therapeutic drugs [16]. In traditional medicine, Triphala is an anticancer agent because it can induce oxidative stress and DNA damage in cancer cells while enhancing immunological responses to inhibit cancer cell proliferation [17]. Additionally, individual herbs like Mudavattukizhangu (*Drynaria quercifolia*) [18], Keezhanelli (*Phyllanthus amarus*) [19], and Karisalankanni (*Eclipta prostrata L*) [20] are listed, each with a composition of 25 grams. These plants have been utilized for millennia and possess therapeutic properties. Trikatu is a blend of three herbs: dried ginger, black pepper (milagu), and long pepper (thippili), utilized as a carminative and purgative and for the treatment of conditions such as obesity, indigestion, and hypothyroidism. Gingerols included in ginger are active molecules that exhibit anticancer properties; for example, they have demonstrated the ability to induce apoptotic death in ovarian cancer cells. Piperine, a principal constituent of black pepper, exhibits many pharmacological effects [21].

Karisalankanni, or *Eclipta prostrata*, is a perennial herb used for dermatological ailments, alopecia, and various skin injuries [22]. It is also used in India, China, and Brazil to treat snake bites; the plant's juice is used to stimulate hair development. *Drynaria quercifolia*, commonly known as Mudavattu kizhangu, is a fern distributed from India to Southeast Asia and Australia [23, 24]. The rhizome has antioxidant, anti-inflammatory, antibacterial, cytotoxic, and various other actions, qualifying it as a multitargeted medicinal agent [25].

Keezhanelli, or *Phyllanthus amarus*, is mainly recognized for its efficacy in addressing gastrointestinal and female reproductive problems, including leucorrhea and menorrhagia [26]. It possesses galactagogue properties and may also be utilized to treat breast abscesses. Triphala, a distinguished Ayurvedic formulation, comprises three botanical species: Amalaki, Bibhitaki, and Haritaki, derived from the fruits of Emblica officinalis, Terminalia bellerica, and Terminalia chebula, respectively. Renowned for its numerous health advantages, Triphala exhibits antioxidant, anti-inflammatory, immunomodulatory, and anticancer effects [27, 28]. The polyherbal formulation generally surpasses traditional treatments paired with herbal formulations by synergistically integrating medicinal ingredients. The synergistic interaction among the compounds enhances therapeutic outcomes, increases medication availability, and diminishes adverse side effects, presenting a promising treatment alternative. Employing our scientific validation of traditional knowledge allows us to integrate herbal and conventional therapies, providing patients with a comprehensive, evidence-based, holistic treatment.

The current study aims to assess the anti-lung cancer efficacy of the polyherbal formulation comprising Thirukadugu, Triphala, Karisalankanni, Mudavattu Kizhangu, and Keezhanelli. This study examines the pharmacological properties of the formulation using lung cancer cells (NCCS-A549) as a model, focusing on its antioxidant, anti-inflammatory, and apoptotic activities. This research seeks to advance the application of plant-based therapeutic options for lung cancer by investigating the synergistic effects of various herbs. The components of the polyherbal formulation utilized in this study are listed in Table 1.

Materials and Methods

Collection of Plant Material

The plants utilized in this study, including Thirukadugu, Triphala, Karisalankanni, Mudavattu Kizhangku, and Keezhanelli, were sourced from the Tirunelveli District of Tamil Nadu. Dr. V. Chelladurai, a former Research Officer in Botany from CCRAS, Government of India, Tirunelveli, identified and certified these plants. Standard

Table 1. Traditional Medicinal Plants and Formulations with Composition Details

S.No	Tamil Name	Common Name	Botanical Name	Composition (gm)
1	Trikatu	Long pepper	*Piper longum*	25
	Equal proportions (1:1:1).	Black pepper	*Piper nigrum*	
		Ginger	*Zingiber officinalis*	
2	Triphala	Amala	*Emblica officinale*	25
	Equal proportions (1:1:1).	Baheda	*Terminaliabellirica*	
		Chebulic myrobalan	*Terminaliachebula*	
3	Mudavattukizhangu		*Drynaria quercifolia*	25
4	Keezhanelli		*Phyllanthusamarus*	25
5	Karisalankanni		*Eclipta prostrata L*	25

ethnobotanical regulations were followed when collecting plant specimens to guarantee correct identification and authentication. Identification drew on morphological traits and cross-referenced with botanical literature and accredited flora databases [29]. Macroscopic and microscopic analysis and phytochemical screening to verify species identification follow World Health Organization (WHO) recommendations for medicinal plant authenticity. The gathered plant specimens were verified to contain no other plant species and were in good condition.

Cell Culture

The A549 lung cancer cell line utilized in this work was acquired from the National Centre for Cell Sciences (NCCS) cell repository in Pune, India [30]. The cells were cultured in Dulbecco's Modified Eagle's Medium (DMEM) supplemented with 10% fetal bovine serum (FBS). To prevent bacterial proliferation during cell cultivation on the spanning medium, supplementary components were incorporated: penicillin at a dosage of 100 U/ml and streptomycin at 100 µg/ml. The cultures were sustained at 37°C in a humidified environment with 5% CO_2 concentration.

Source of Chemical and Reagents

The chemicals utilized in this investigation comprise Dulbecco's Modified Eagle's Medium (DMEM), streptomycin, penicillin-G, L-glutamine, phosphate-buffered saline (PBS), and 3-(4,5-dimethylthiazol-2-yl)-2,5-diphenyltetrazolium bromide (MTT). Additional reagents such as dimethyl sulfoxide (DMSO), Folin-Ciocalteu reagent, sodium carbonate, aluminum chloride, sodium nitrite, sodium hydroxide, sulfuric acid, ferric chloride, chloroform, and various solvents (methanol, hexane, ethyl acetate, and water) were used for phytochemical analysis and antioxidant assays. The study also employed 2,2-diphenyl-1-picrylhydrazyl (DPPH), molybdate, sodium phosphate, diclofenac, acridine orange (AO), and ethidium bromide (EB) for biochemical and cytotoxicity tests. All chemicals utilized in this investigation were of analytical quality and procured from HiMedia Laboratories Private Limited, India.

Extraction of Samples

Five plants were selected, gathered, and washed to eliminate dust and debris without applying pressure. A maceration technique, as described in [31], was conducted. The plant materials were dried, crushed, and soaked in distilled water at 40°C with occasional stirring. The extract was then filtered and concentrated by evaporation to obtain a dry residue for further analysis.

Phytochemical Qualitative Analysis

The plant extracts were subjected to qualitative screening following standard phytochemical protocols as described in [32]. Dragendorff's reagent was used to identify alkaloids; flavonoids were identified with sodium hydroxide, terpenoids with chloroform and sulfuric acid, and glycosides with Borntrager's test. The foam test turned up saponins and ferric chloride-verified phenols. Fehling's test identified carbohydrates, proteins, and amino acids, which were evaluated using the Biuret and Ninhydrin assays accordingly [33].

Quantitative Analysis

The Folin-Ciocalteu approach was used to ascertain the total phenolic content; five separate solvents were extracted, and then spectrophotometric analysis was performed at 650 nm [34]. Using a modified spectrophotometric technique, the flavonoid amount was calculated and reported as quercetin equivalents; absorbance was measured at 510 nm [35]. The phosphomolybdenum test evaluated antioxidant activity; extracts were incubated at 95°C under molybdate, sodium phosphate, and sulfuric acid, and absorbance was noted at 695 nm [36]. The antioxidant capability was assessed using the DPPH radical scavenging test; absorbance was measured at 517 nm to ascertain % inhibition [37, 38]. Every technique used accepted conventions as detailed in the corresponding sources.

Membrane Stabilization Test

The membrane stability test was carried out with few changes, as detailed in [39]. Fresh human blood was briefly collected in heparinized tubes, processed to produce a 10% red blood cell solution, and then treated with the plant extract. Saline was the negative control; diclofenac was the positive control. The reaction mixtures were centrifuged after incubation at 56°C and then evaluated for absorbance at 560 nm to evaluate membrane stability.

MTT Assay

The viable A549 cells were plated onto a hemocytometer for enumeration. The cells were seeded at a 1×10^4 cells/mL density in 96-well plates and permitted to adhere for 24 hours. Subsequently, the cells were administered the sample at 50, 100, 200, and 500 µg/mL doses in each well. The treated cells were placed in a fresh incubator at 37°C with 95% humidity and 5% CO_2 for 24 hours. After incubation, the cells were rinsed with fresh culture medium to eliminate the treatment and were subsequently exposed to MTT dye (5 mg/mL in PBS) for 4 hours at 37°C. The purple formazan crystals were subsequently dissolved in 100 µL of pure DMSO. Viability was assessed by measuring absorbance at 540 nm using a multi-well plate reader to confirm the efficacy of the treatments [40]. The percentage of live cells was determined relative to the control, and the IC_{50} value was calculated.

Inhibition of cell Polifereation (%)=(Mean AB of Control-Mean AB of the Sample)/(Mean AB of the Control)×100

Measurement of Apoptotic Induction

A549 cells were grown in 6-well plates at a density of 5×10^4 cells per well for 24 hours to facilitate cell attachment. A549 cells are commonly employed in scientific research as a model for lung cancer due to their comprehensive characterization, epithelial shape, and capacity to evaluate medication efficacy and oxidative stress responses [41]. The A549 cell line is distinguished by its functioning p53 proteins and is ideal for assessing

apoptosis and cytotoxicity of therapeutic medicines compared to other lung cancer cell lines such as H1299 and H460 [42]. After 24 hours of treatment with plant extracts at concentrations of 100 and 150 µg/mL, the cells were detached, rinsed with cold PBS, and stained with acridine orange (AO) and ethidium bromide (EB) in a 1:1 ratio (100 µg/mL each), followed by incubation at 25°C for 5 minutes. The dyed cells were subsequently examined using a fluorescent microscope 20X to assess morphological alterations. Upon completion of the treatment, cells were harvested, subjected to three washes with PBS, and subsequently stained with the AO/EB dye mixture (100 µg/mL, 1:1 ratio) for 5 minutes. The stained cells were subsequently examined using a fluorescent microscope at 40x magnification. Apoptotic cells were enumerated relative to the overall cell count in each recorded microscopic field [43].

Molecular Docking

This work employed molecular docking via AutoDock Vina to assess 13 phytochemicals' capacity to inhibit the Epidermal Growth Factor Receptor (EGFR) tyrosine kinase domain (PDB ID: 1M17) [44, 45]. The 3D structure of the phytochemicals was acquired from PubChem and subjected to energy minimization using Open Babel software [46]. The EGFR tyrosine kinase receptor structure was also constructed for the docking study. The docking process in AutoDock Vina required the definition of the search space using a grid box of 60 Å along each of the three axes. Subsequent docking simulations were conducted, and the resultant poses were assessed by computing binding affinities. The poses that achieved the highest rankings were selected for additional investigation. The fidelity of the receptor-ligand interaction and their binding modalities were further evaluated by molecular docking analysis and visualization with PyMOL [47].

Molecular Dynamics

The analysis of trajectories obtained from molecular dynamics (MD) simulations provided insights into the stability of the complex, its conformational adaptability, its compactness, and its interactions with the solvent. This study utilized MD simulations conducted with the GROMACS software tool [48]. The procedure commenced with energy reduction of the protein-ligand complex in a vacuum using the steepest descent algorithm. This method involved refining atomic coordinates iteratively to determine the system's minimal potential energy. Following minimization, the complex was placed in a periodic water box with the SPC water model, which serves as a reference for more intricate water models [49]. The physiological conditions were sustained by incorporating sodium and chloride ions to attain a concentration of 0.15 M. The solvated system was equilibrated under the NPT ensemble and subsequently underwent a 100 ns production run under the same ensemble. It ensured that the simulation conditions incorporated biological or physiological reality. Post-simulation, the trajectory data was examined using GROMACS tools to assess structural and dynamic properties.

Binding free energy calculations

MMPBSA simulations were conducted to evaluate the binding energies of ligands to the EGFR tyrosine kinase domain [50]. The interactions between the receptor and the ligands STD, DRG1, and DRG2 were analyzed using the final 50 ns of the GROMACS simulation trajectories. Before executing MMPBSA, the complexes were solvated, and topology files were generated in GROMACS. The investigations conducted using the g_MMPBSA program elucidated the disaggregation of energy contributions to ascertain binding affinities and delineate interaction hotspots.

Results

Phytochemical Qualitative Analysis

The sample's phytochemical screening showed several bioactive compounds, thus supporting the plant's functional claim (Table 2). Indicating possible pharmacological and nutritional value, the qualitative study verified the presence of alkaloids, phenols, flavonoids, glycosides, proteins, carbs, and fixed oils. While glycosides may have cardiac or laxative effects, alkaloids and flavonoids point to antioxidant and antibacterial qualities. A lack of terpenoids, saponins, and amino acids might lower the anti-inflammatory or anticancer effects. The phytochemical profile, taken as a whole, emphasizes the extract's bioactive power.

DPPH Free Radical Scavenging Assay

Table 3 supports the premise that the tested compound has a high percentage of inhibition by showing a dose-dependent relationship. However, percentage inhibition was the lowest at 10.25% at the lowest concentration of 20 µg/mL and increased steeply to 46.15% for 40 µg/mL and 49.89% for 60 µg/mL. This trend was sustained with 57.69% inhibition at 80 µg/mL maximum inhibition of 69.23% at 100 µg/mL. The cytotoxicity concentration, computed as 60.13 µg/mL, represents the value corresponding to 50% inhibition.

Table 2. Phytochemical Screening of the Sample Showing the Presence or Absence of Various Bioactive Compounds based on Specific Tests and Reagents.

Phytochemical Test	Reagents	Inference
Alkaloids	Dragendorff's test	Present
Phenols	Ferric chloride test	Present
Flavonoids	Alkaline reagent test	Present
Terpenoids	Skawolki's test	Absent
Glycosides	Borntrager's test	Present
Saponins	Foam test	Absent
Proteins	Biuret test	Present
Amino acids	Ninhydrin test	Absent
Carbohydrates	Fehling's test	Present
Fixed oil	Spot test	Present

Phosphomolybdenum Assay

Table 4 supports the premise that the tested compound has a high percentage of inhibition by showing a dose-dependent relationship. However, percentage inhibition was the lowest at 10.25% at the lowest concentration of 20 µg/mL and increased steeply to 46.15% for 40 µg/mL and 49.89% for 60 µg/mL. This trend was sustained with 57.69% inhibition at 80 µg/mL maximum inhibition of 69.23% at 100 µg/mL. The cytotoxicity concentration, computed as 60.13 µg/mL, represents the value corresponding to 50% inhibition. This result implies that the compound has moderate activity, and its inhibitory properties are enhanced with increased compound concentration. The results also indicate that the compound could be further examined for therapeutic efficacy.

Anti-inflammatory Assay

Table 5 shows a dose-dependent response where the percentage inhibition increases with the concentration of the compound. The compound at a concentration of 20 µg/mL showed 23.51 % inhibition, which increased as the compound's concentration increased. The inhibition increased to 31.42% at 40 µg/mL and reached 39.66% at 60 µg/mL. This trend was also maintained with additional enhancement to 47.31% at 80µg/ml and 59.67% at the highest 100µg/ml concentration. These results indicate that the compound has a significant inhibitory activity that increases with its concentration.

Heavy metal analysis

According to Table 6, the percentage of inhibition increases proportionally with the concentration of the compound. At a concentration of 20 µg/mL, the compound showed 23.51% inhibition, which went up as the concentration did. At 40 µg/mL, it rose to 31.42%; at 60 µg/mL, it reached 39.66%. This trend continued to increase to 47.31% at 80µg/ml and 59.67% at the highest 100µg/ml concentration. These results show that the compound has a dose-dependent inhibitory effect. The precise and progressive nature of the inhibition seen in this study confirms that the compound could be helpful for further research into its inhibitory properties and potential for use in clinical settings.

GC-MS Analysis

Figure 1 is a chromatogram derived from electron ionization (EI) mass spectra, with time (minute) on the abscissa and ion density on the ordinate. Here, the sample's compounds elute at retention times of 5.736 min, 7.343 min, 10.105 min, 17.138 min, and 26.637 min. The highest peak, indicated by an asterisk, at 26.637 minutes. The retention times vary from 5.194 to 26.637 min and are correlated with chemical classes of fatty acids, esters, hydrocarbons, and other bioactive compounds. Noted

Table 3. Dose- Dependent Percentage Inhibition of the Compound and its IC_{50} Value, Highlighting Its Inhibitory Activity Across Varying Concentrations.

Concentration (µg/mL)	Percentage Inhibition
20	10.25
40	46.15
60	49.89
80	57.69
100	69.23
IC_{50}	60.13 µg/mL

Table 4. Dose-dependent Percentage Inhibition of the Compound by Phosphomolybdenum Assay, Showing Increasing Inhibitory Activity with Higher Concentrations

Concentration (µg/mL)	Percentage Inhibition
20	0.521
40	0.869
60	1.048
80	1.293
100	1.367

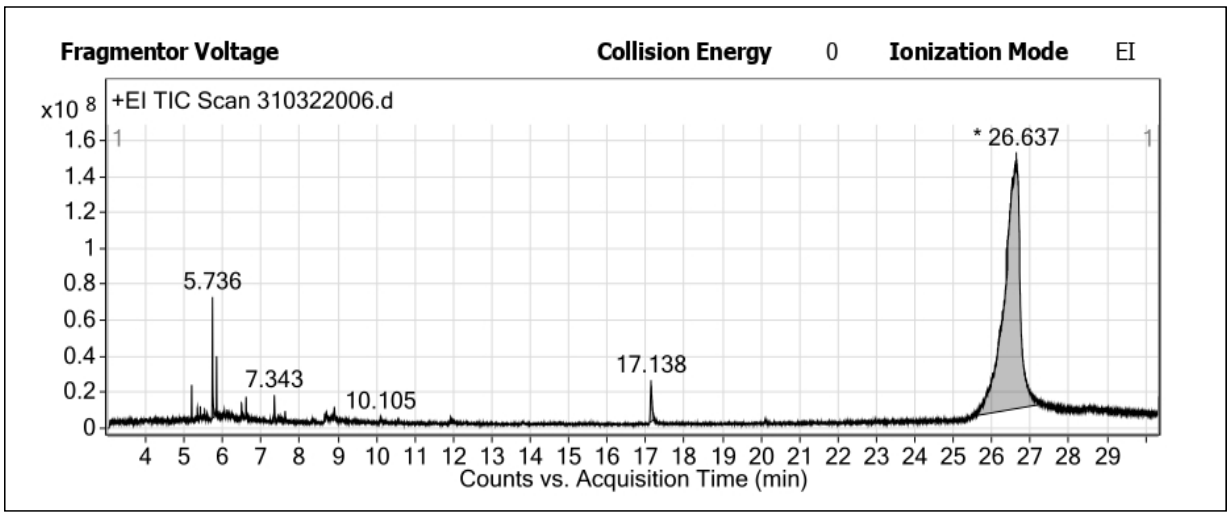

Figure 1. GC-MS Chromatogram Indicating Distinct Peaks at Retention Times of 5.736, 7.343, 10.105, 17.138, and 26.637 minutes, with the most prominent peak at 26.637 minutes, indicating the presence of various compounds in the sample.

molecules include Dodecanoic acid (RT = 5.736), a fatty acid, and Trimyristin (RT = 26.637), a triglyceride and the most dominant peak in the chromatogram. The table shows structural variations, like bicyclic compounds like Bicyclo[5.2.0]nonane and long chain fatty acids like Icosapent, eluting at three different retention times, 5.589, 6.118, and 11.998. Other bioactive molecules include Piperine (RT = 17.138), a spice and therapeutic compound, and Gamolenic Acid (RT = 11.94), an essential fatty acid. Identifying esters, including Hexadecanoic acid and ethyl ester (RT = 7.626), shows that derivatization has occurred or that the ester is naturally present.

Cell Culture-based Test

The results presented in Figure 2 revealed the cytotoxicity of the polyherbal extract on A549 lung cancer cells for 24 hours of the treatment period in terms of morphology and quantitative analysis of cell viability and inhibition. In Figure 2A, the changes in the A549 cell morphology after the treatment with the polyherbal extract at a concentration of 150 µg/ml and 200 µg/ml were compared to the control group. The control cells appear healthy and homogenous with low levels of apoptosis. However, treated cells exhibit typical changes in cell morphology, including cell shrinkage and low cell density, suggesting cytotoxicity at elevated extract concentrations. These modifications indicate the possible activation of cell death programs, such as apoptosis or necrosis.

Figure 2B demonstrates the trend of the concentration-dependent inhibition of the polyherbal extract, where

Table 5. Dose- Dependent Percentage Inhibition of the Compound Across Various Concentrations by Anti-Inflammatory Assay, Demonstrating Its Inhibitory Potential

Concentration (µg/mL)	Percentage Inhibition
20	23.51
40	31.42
60	39.66
80	47.31
100	59.67

Table 6. Heavy Metal Analysis of the Sample, Showing Concentrations of Various Elements and Their Quantification Status.

S.No	Parameter	Results (mg/kg)	Test
1	Manganese	17.43	HECS/INS/SOP/013
2	Antimony	13.36	HECS/INS/SOP/013
3	Molybdenum	22.51	HECS/INS/SOP/013
4	Selenium	BLQ (LOQ:0.1)	HECS/INS/SOP/013
5	Arsenic	BLQ (LOQ:0.1)	HECS/INS/SOP/013
6	Cadmium	BLQ (LOQ:0.1)	HECS/INS/SOP/013
7	Chromium	0.487	HECS/INS/SOP/013
8	Copper	BLQ (LOQ:0.1)	HECS/INS/SOP/013
9	Mercury	BLQ (LOQ:0.1)	HECS/INS/SOP/013
10	Nickel	1.06	HECS/INS/SOP/013
11	Lead	BLQ (LOQ:0.1)	HECS/INS/SOP/013
12	Zinc	0.928	HECS/INS/SOP/013
13	Tin	BLQ (LOQ:0.1)	HECS/INS/SOP/013
14	Iron	32.24	HECS/INS/SOP/013
15	Vanadium	BLQ (LOQ:0.1)	HECS/INS/SOP/013
16	Aluminium	11.05	HECS/INS/SOP/013

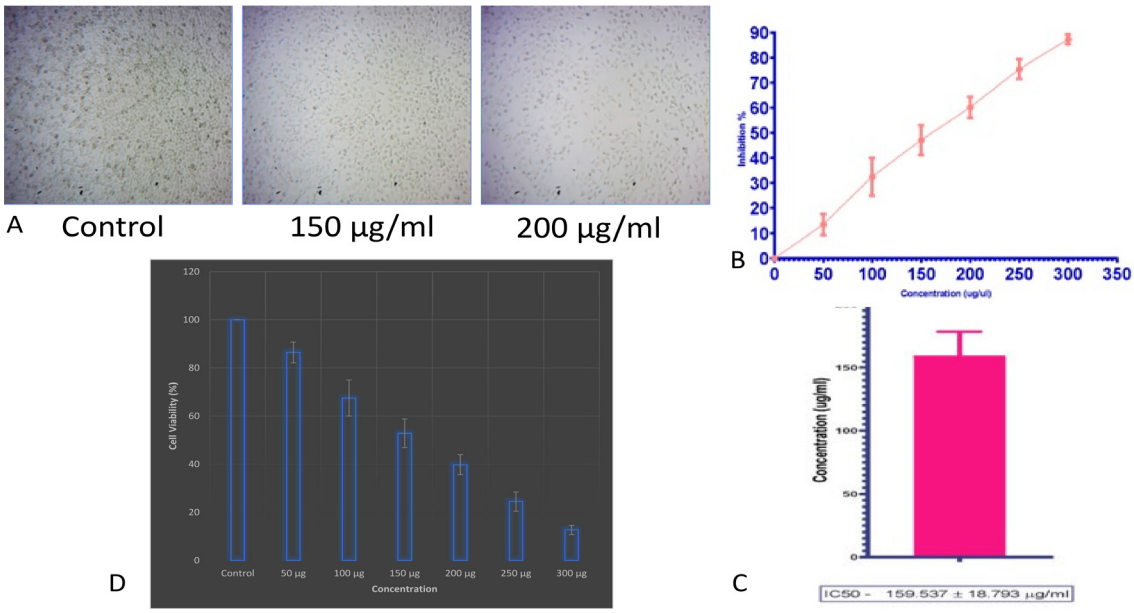

Figure 2. Effects of Polyherbal Extract on A549 Lung Cancer Cells. (A) Morphological changes observed in untreated control cells and cells treated with 150 µg/ml and 200 µg/ml of the extract for 24 hours, showing reduced cell density and structural alterations. (B) Dose-response curve illustrating the percentage inhibition of A549 cells at increasing extract concentrations, demonstrating a concentration-dependent inhibitory effect. (C) Determination of the IC_{50} value, calculated as 159.54 ± 18.79 µg/ml, indicating the extract's potency. (D) Cell viability assay showing a significant decrease in cell viability with increasing concentrations of the extract. Error bars represent the standard deviation from three independent experiments.

the level of inhibition increases with an increase in the concentration of the extract. The graph shows a straight-line relationship; thus, more extract concentration inhibits the growth of the A549 cell line. This data also corroborates the hypothesis that the extract has a dose-dependent anticancer effect. In the Figure 2C, the IC_{50} value was estimated to be approximately 159.54 ± 18.79 µg/ml. The IC_{50} is defined as the concentration of the polyherbal extract that caused cell growth inhibition by 50%. This value is one of the essential factors for determining the concentration and activity of the extract concerning the inhibition of lung cancer cell proliferation. The low IC_{50} value indicates higher cytotoxicity of the extract against A549 cells compared to the other investigated cell lines. Figure 2D supports the cytotoxicity data through a cell viability assay. The bar graph shows that cell viability decreases with extract concentrations and more evidently at concentrations higher than 100 µg/ml. At the highest concentration of the tested compound (300 µg/ml), the level of cell viability is significantly reduced, which confirms the strong anticancer potential of the given substance. In all figures, error bars denote standard deviations, which underscore the repeatability and statistical validity of the results.

Apoptotic activity

The polyherbal formulation shown in Figure 3 also depicts the two biological functions of the formulation, which are the apoptotic activity on the A549 lung cancer cells. In the upper panel of the figure, fluorescence microscopy shows that green fluorescence was observed in control cells, indicating viable cells. In contrast, cells treated with 150 µg/ml and 200 µg/ml of the formulation showed increased red fluorescence indicative of apoptotic or necrotic cell death in a dose-dependent manner. This goes well with the formulation that the compound triggers apoptosis, which is an essential component of cancer therapies.

Molecular Docking

Table 7 shows the docking scores and interaction affinities of the phytochemicals concerning Erlotinib, the standard drug against Epidermal Growth Factor Receptor (EGFR) tyrosine kinase. The docking scores in kcal/mol are distinctly provided in the table, where a lower score correlates with more favorable binding interaction. The data show that several phytochemicals may possess EGFR inhibitory activity. The standard drug Erlotinib, a widely used EGFR tyrosine kinase inhibitor, provides the highest docking score of -8.1 kcal/mol to the target site and is used as the reference. Among the phytochemicals, Piperine has the highest binding energy of -7.9 kcal/mol, a value very close to the standard. It can be inferred to be a potential competitive EGFR inhibitor. Due to its advantageous properties, the therapeutic efficacy of Piperine exceeds that of Erlotinib in terms of binding

Table 7. Docking Score and Type of Interaction of Phytochemical against Epidermal Growth Factor Receptor Tyrosine Kinase

S.NO	Ligand	ID	Affinity kcal/mol
1	Erlotinib [STD]	176870	-8.1
2	Piperine [Top1]	638024	-7.9
2	2-Cyclohxyl-2,5-cyclohexadiene [Top2]	586143	-7.5
4	Bicyclo (5,2.0) nonane 2-methylene-4,8,8-trimethyl-4-vinyl	564746	-7.1
5	Icosapent	446284	-6.3
6	Naphthalene, decahydro-1,1-dimethyl	557347	-6.3
7	Methyl 9,11-Octadecadiynoate	14957561	-6
8	Gamolenic acid	5280933	-6
9	2,5-Octadecadiynoic acid, methylester	42151	-5.9
10	Hexadecanoic acid, ethylester	12366	-5.4
11	Tetra decanoic acid	11005	-5.2
12	Dodecanoic acid	3893	-5.1
13	Cis-Vaccenic acid	5282761	-4.9

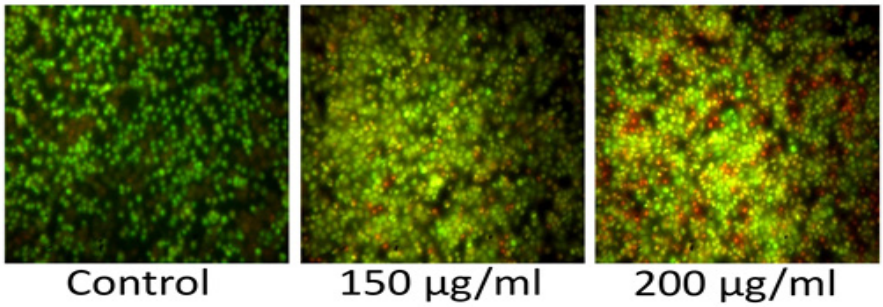

Figure 3. Effect of Polyherbal Formulation on the Apoptotic Cell Death in the Lung Cancer A549 Cells.

ability. Piperine exhibits enhanced safety characteristics and less toxicity, increasing its overall cost-effectiveness relative to synthetic inhibitory agents in medical applications. Piperine enhances medication bioavailability when co-administered with other therapies and exhibits synergistic benefits with many anticancer agents, hence improving treatment outcomes [51]. Experimental research indicates that Piperine may function as an adjunct or alternative in lung cancer therapy. The second-ranked phytochemical, 2-Cyclohexyl-2,5-cyclohexadiene, is estimated to have a docking score of -7.5 kcal/mol, and the second but one compound, Bicyclo (5,2.0) nonane 2-methylene-4,8,8-trimethyl-4-vinyl, a docking score of -7.1 kcal/mol. The other groups of phytochemicals also show moderate binding energies, which lie between -6.3 and -6 kcal/mol: Icosapent, Naphthalene, decahydro-1,1-dimethyl, and Methyl 9,11-Octadecadiynoate. Although not as active as Piperine and the superior ligands, these compounds demonstrate reasonable potency in reducing EGFR activity. As expected, the compounds such as Hexadecanoic acid, ethylester, Tetradecanoic acid, and Dodecanoic acid have low binding affinities of between -5.4 and -5.1 Kcal/mol. The lowest affinity is recorded at Cis-Vaccenic acid, for which the energy value obtained is -4.9 kcal/mol, thus suggesting poor binding with the receptor.

The binding modes and possible inhibitory mechanisms of lead phytochemicals and standard inhibitors are shown in Figure 4, representing the molecular interactions of phytochemicals with human salivary amylase enzyme at the active site. The binding pose of Miglitol, a standard inhibitor, is shown in Figure 4A. Miglitol forms hydrogen bonds and hydrophobic contacts with key amino acid residues such as LEU 694, VAL 702, THR 766, and LYS 721. The binding pose of another standard inhibitor, Acarbose, is depicted in the figure 4B. Acarbose interacts with side chain residues through hydrogen bonding; it forms hydrogen bonds with the amino acid residues of THR 830, ASP 831, LYS 721, and MET 742, while hydrophobic interactions.

Figure 4C shows the binding pose of the phytochemical 1HE, which has an almost similar interaction pattern to the standard inhibitors. Positions Val702, Met 769, Thr 830, and Asp 831 are crucial to its proper positioning within the active site. However, multiple hydrogen bond formation due to two hydroxyl groups in the structure makes it more potent as an inhibitor. In Figure 4D, it is clearly shown that C4B has lesser interaction than Miglitol, Acarbose, and 1HE. The interaction primarily consists of residues such as ALA 719, VAL 702, and MET 742, which gives a weak binding affinity. The figure demonstrates that Miglitol and Acarbose have high binding affinities due to interactions with multiple active site residues.

Molecular Dynamics Simulations

Figure 5 illustrates the structural dynamics and stability analysis of apo 1M17, 1M17-STD, 1M17-DRG1, and 1M17-DRG2 under molecular dynamics simulations. The metrics examined include root mean square deviation (RMSD), root mean square fluctuation (RMSF), radius of gyration (Rg), solvent-accessible surface area (SASA), hydrogen bonding, and corresponding RMSD trends.

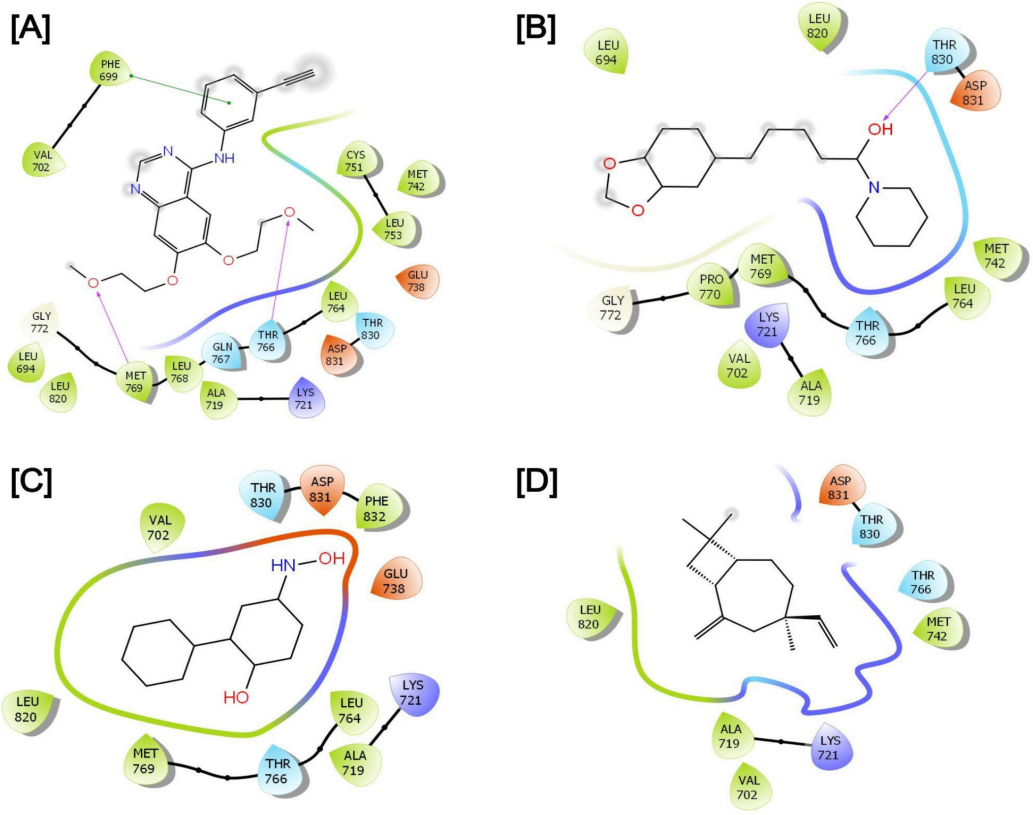

Figure 4. Interaction of Lead Phytochemicals and Standard Inhibitor at the Human Salivary Amylase Active Site. (A) Binding pose of Miglitol (B) Binding pose of Acarbose(C) Binding pose of 1HE (D) Binding pose of C4B.

The top panel depicts RMSD (Figure 5A) and RMSF (Figure 5B) analyses. The RMSD plot indicates that the apo form and its drug-bound counterparts exhibit structural stability, with minor deviations over the simulation time. However, 1M17-STD shows slightly higher fluctuations, suggesting that the standard compound may introduce greater flexibility. The RMSF plot further highlights the residue-specific fluctuations, with notable peaks around residues 750–850, indicative of localized flexibility in this region.

The middle panel presents the Rg (Figure 5A) and SASA (Figure 5B) analyses. The Rg values remain relatively consistent across all systems, with minimal variation over the simulation time, indicating preserved compactness of the protein structure. The SASA plot demonstrates that the apo form has a slightly lower surface area than drug-bound forms, implying that ligand binding may induce minor conformational changes that alter the solvent-exposed surface. Among the drug-bound systems, differences in SASA values between 1M17-DRG1 and 1M17-DRG2 suggest variations in ligand interactions and their effects on protein conformation. The bottom panel focuses on hydrogen bonding (Figure 5A) and the corresponding RMSD trends (Figure 5B). The hydrogen bond plot reveals that the ligand-bound systems form stable hydrogen bonds throughout the simulation, with 1M17-DRG1 and 1M17-DRG2 showing a slightly higher number of hydrogen bonds than 1M17-STD. This observation suggests stronger or more stable interactions with these ligands. The corresponding RMSD trends align with these findings, as the lower RMSD values for 1M17-DRG1 and 1M17-DRG2 compared to 1M17-STD further confirm their stabilizing effect on the protein structure.

Binding Free Energy of Complexes

In the binding energetics, 1M17-DRG2 has the highest binding energy and the highest polar solvation but the lowest van der Waal and electrostatic energies, suggesting that 1M17-DRG2 has the strongest binding to the protein of the four compounds (Table 8). As expected, 1M17-STD and 1M17-DRG1 show less binding affinities, and less

Table 8. Binding Energetics of 1M17-STD, 1M17-DRG1, and 1M17-DRG2, Including van der Waals Energy, Electrostatic Energy, Polar Solvation Energy, and Net Binding Energy, Presented as mean ± standard deviation

Complexes	van der Waal energy	Electrostatic energy	Polar salvation energy	Binding energy
1M17-STD	-81.212 +/- 55.151 kJ/mol	-17.563 +/- 16.140 kJ/mol	93.356 +/- 78.204 kJ/mol	-17.216 +/- 40.876 kJ/mol
1M17-DRG1	-42.644 +/- 33.984 kJ/mol	-16.780 +/- 18.621 kJ/mol	50.995 +/- 44.777 kJ/mol	-14.253 +/- 47.513 kJ/mol
1M17-DRG2	-85.759 +/- 10.046 kJ/mol	-58.308 +/- 19.144 kJ/mol	117.203 +/- 23.569 kJ/mol	-39.235 +/- 13.531 kJ/mol

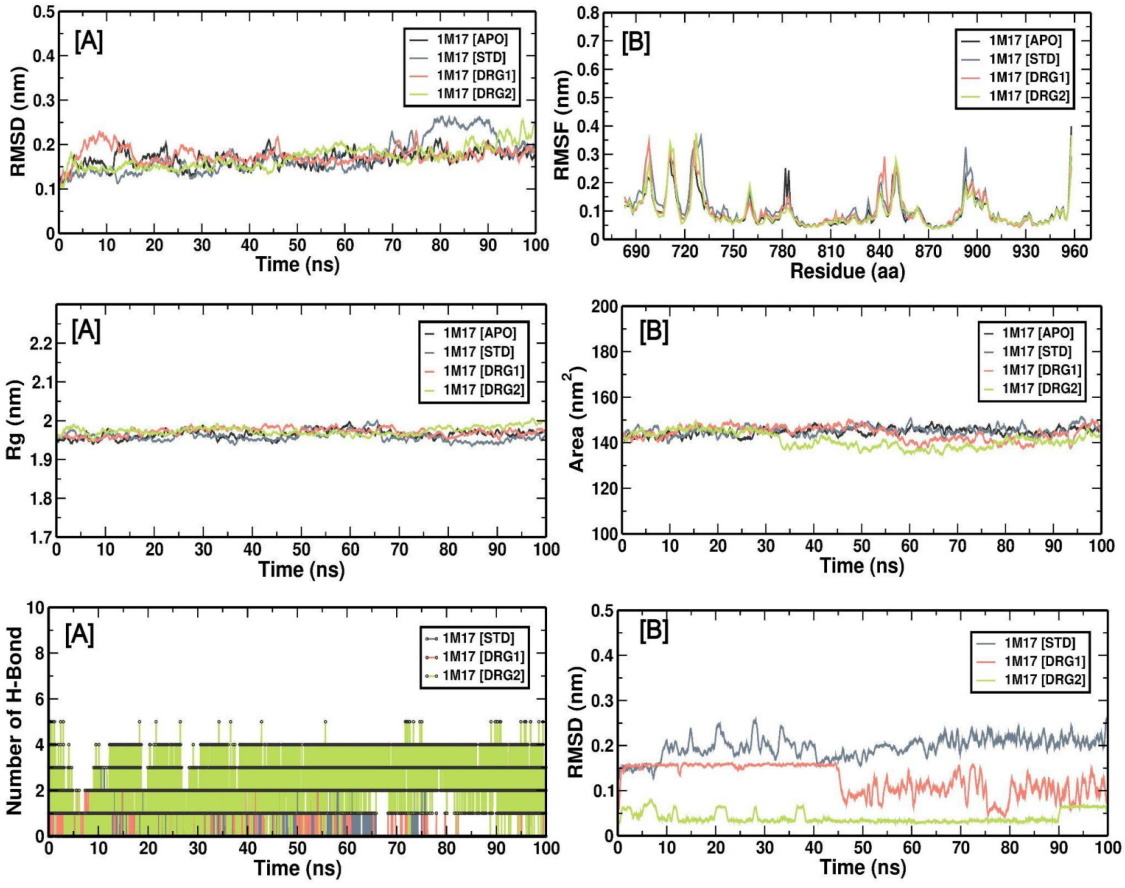

Figure 5. RMSD and RMSF Values of apo 1M17, 1M17-STD, 1M17-DRG1 and 1M17-DRG2 (top panel); Rg values and time-area plot of apo 1M17, 1M17-STD, 1M17-DRG1 and 1M17-DRG2 (middle panel); Hydrogen bond numbers and its corresponding RMSD of apo 1M17, 1M17-STD, 1M17-DRG1 and 1M17-DRG2 (bottom panel).

favorable van der Waals and electrostatic energies, which correspond to higher and less stable binding energies (-17.216 ± 40.876 kJ/mol and -14.253 ± 47.513 kJ/mol). The present outcome has revealed that the 1M17-DRG2 ligand has more excellent stability and stronger binding affinity than other ligands considered in the study; therefore, it is more suitable for use in therapies.

Discussion

This work aimed to assess the therapeutic potential of a polyherbal extract (Thirukadugu, Triphala, Karisalankanni, Mudavattu Kizhangu, and Keezhaneli) for lung cancer. With molecular docking and dynamics simulations to ascertain its efficacy as an EGFR tyrosine kinase inhibitor, the extract was evaluated for its phytochemical content and antioxidant, anti-inflammatory, antibacterial, and anticancer effects. The results suggest the need for further research on the therapeutic uses of the bioactive chemicals as they provide insightful analysis of their possible target in lung cancer.

Phytochemical analyses revealed the presence of alkaloids, phenols, flavonoids, glycosides, proteins, carbohydrates, and fixed oils; however, terpenoids, saponins, and amino acids were not identified. The quantitative analysis indicated total phenols at 0.464 mg QE and flavonoids at 0.324 mg GAE, which may account for the extract's biological effects. The DPPH free radical scavenging assay results indicate that the extract exhibits significant antioxidant activity, evidenced by an IC_{50} value of 60.13 µg/mL, demonstrating its efficacy in scavenging free radicals. Moreover, the phosphomolybdenum assay corroborated the total antioxidant capability, showing an increased concentration factor for both inhibition % and absorbance. The anti-inflammatory assay was promising, suggesting that the extract may affect inflammation pathways, possibly due to its phenolic and flavonoid content, which is known for its anti-inflammatory properties [52]. Consequently, the extract's ability to inhibit the synthesis of pro-inflammatory mediators warrants further investigation to elucidate its molecular actions.

Phytochemicals identified with pharmacological activity include those analyzed by gas chromatography-mass spectrometry (GC-MS). Piperine and 2-cyclohexyl-2,5-cyclohexadiene exhibited the highest binding affinities of -7.9 kcal/mol and -7.5 kcal/mol, respectively, to the EGFR tyrosine kinase domain in the docking analysis. The findings approximated the reference inhibitor Erlotinib (-8.1 kcal/mol), suggesting that these phytochemicals could serve as potential EGFR inhibitors. Additional compounds comprised bicyclo(5,2.0)nonane 2-methylene-4,8,8-trimethyl-4-vinyl, exhibiting moderate binding energies (-7.1 kcal/mol) alongside fatty acid derivatives, which displayed lower binding energies than the other compounds. The finding of high-affinity ligands indicates the potential of utilizing the extract as a source of EGFR-targeting compounds [53]. Piperine is a renowned alkaloid from Piper nigrum. It is easily obtained, and commercially scaled synthesis or extraction is possible. Less research has been done on 2-cyclohexyl-2,5-cyclohexadiene and bicyclo(5,2.0) nonane derivatives, yet because of restricted natural sources and possible synthetic complexity, they could provide difficulties in large-scale manufacture. More investigation on affordable synthesis pathways or efficient extraction techniques would be required to investigate their viability for pharmacological uses.

The dependability of the docking results was additionally corroborated by molecular dynamics (MD) simulations, which demonstrated the stability of the protein-ligand complexes. The stabilization was mainly achieved by hydrogen bonding, which was then corroborated by trajectory analysis. Among all evaluated complexes, the most excellent stability was noted for 1M17-STD (Erlotinib) and the 1M17-DRG1 (Piperine) and 1M17-DRG2 (2-Cyclohexyl-2,5-cyclohexadiene) complexes. The MM-PBSA analysis offered additional evidence of the advantageous interactions in the three complexes, while the residue-level energy profile enhanced the comprehension of the stabilizing factors. Consequently, these findings suggest that the phytochemicals found in the extract may serve as possible alternatives or adjuncts to existing EGFR inhibitors in cancer therapy.

The cell culture experiments utilizing A549 cells corroborated the extract's anticancer efficacy. Typical signs of apoptosis, such as cell shrinkage, membrane blebbing, and nuclear condensation, were observed in the treated cells. Fluorescence microscopy of AO/EB labeling revealed early and late apoptotic stages, with treated cells exhibiting yellow and orange hues. This study's findings indicate that the extract can specifically induce apoptosis in cancer cells, a crucial element in cancer therapy. Although our investigation offers critical new perspectives on the possible anticancer effects of the polyherbal formulation, some constraints have to be admitted. Our studies, carried out using a single lung cancer cell line (A549), have in vitro character, which may restrict the generalizability of the results to other lung cancer subtypes or in vivo circumstances. Furthermore, even if they help to forecast binding interactions, molecular docking studies need more confirmation via comprehensive biochemical and in vivo experiments to verify the therapeutic possibilities of the discovered molecules. Future studies should concentrate on assessing the formulation across several cancer cell lines, performing in vivo efficacy and toxicity tests, and investigating clinical application, thus increasing our results' translational significance.

In conclusion, the evaluated herbal extract exhibits diverse biological activities, including antioxidant, anti-inflammatory, antibacterial, and anticancer properties. The existence of other active compounds exhibiting significant interaction with EGFR suggests its potential as a source for novel pharmaceuticals. Consequently, additional in vivo investigations and clinical evaluations are required to validate the extract's efficacy and non-toxicity in therapeutic applications. This study's integration of computational and experimental methodologies demonstrates that multidisciplinary approaches are essential in natural products and drug development.

Author Contribution Statement

Concept: RL, TA, JS, Design: KMS, KP, Experimental Studies: MYA, SV, AC, Data analysis: KMS, Statistical analysis: RL, TA Manuscript preparation: TA, JS. All authors read and approved the final manuscript

Acknowledgements

Approval

The study protocol was approved by the Institutional Review Board (or Ethics Committee) of Sri Ramachandra Institute of Higher Education and Research, Chennai.

Declaration of Interests

The authors declare that they have no competing financial or any other conflict of interests that could have appeared to influence the work reported in this paper.

Ethics Committee Approval

The study protocol was approved by the Institutional Review Board (or Ethics Committee) of Sri Ramachandra Institute of Higher Education and Research, Chennai.

References

1. Leiter A, Veluswamy RR, Wisnivesky JP. The global burden of lung cancer: current status and future trends. Nat Rev Clin Oncol. 2023;20(9):624–39. https://doi.org/10.1038/s41571-023-00798-3
2. Liao KM, Lee CS, Wu YC, Shu CC, Ho CH. Prior treated tuberculosis and mortality risk in lung cancer. Front Med. 2023;10:1121257. https://doi.org/10.3389/fmed.2023.1121257
3. Inage T, Nakajima T, Yoshino I, Yasufuku K. Early Lung Cancer Detection. Clin Chest Med. 2018;39(1):45–55. https://doi.org/10.1016/j.ccm.2017.10.003
4. Daniel VS, Daniel TM. Old Testament Biblical References to Tuberculosis. Clin Infect Dis. 1999;29(6):1557–8. https://doi.org/10.1086/313562
5. Shojaei S, Pourmadadi M, Homayoonfal M, Behnamrad P, Fathi-karkan S, Rahdar A, et al. Revolutionizing lung cancer treatment: Nanotechnology-driven advances in targeted drug delivery and novel therapeutic strategies. J Drug Deliv Sci Technol. 2024;101:106186. https://doi.org/10.1016/j.jddst.2024.106186
6. Sundaram KKM, Bupesh G, Saravanan KM. Instrumentals behind embryo and cancer: a platform for prospective future in cancer research. AIMS Mol Sci. 2022;9(1):25–45. https://doi.org/10.3934/molsci.2022002
7. Rina A, Maffeo D, Minnai F, Esposito M, Palmieri M, Serio VB, et al. The Genetic Analysis and Clinical Therapy in Lung Cancer: Current Advances and Future Directions. Cancers. 2024;16(16):2882. https://doi.org/10.3390/cancers16162882
8. Jha S, Vaiphei KK, Alexander A. Chapter 1 - Plant-based therapeutics: current status and future perspectives. In: Singh MR, Singh DBT-P and HD, editors. Academic Press; 2023. p. 3–11. Available from: https://www.sciencedirect.com/science/article/pii/B9780323991254000032
9. Patwardhan K, Pathak J, Acharya R. Ayurveda formulations: A roadmap to address the safety concerns. J Ayurveda Integr Med. 2017;8(4):279-82. https://doi.org/10.1016/j.jaim.2017.08.010.
10. Moussavi N, Mounkoro PP, Dembele SM, Ballo NN, Togola A, Diallo D, et al. Polyherbal Combinations Used by Traditional Health Practitioners against Mental Illnesses in Bamako, Mali, West Africa. Plants. 2024;13(3):454. https://doi.org/10.3390/plants13030454
11. Wagner H. Synergy Research: A New Approach to Evaluating the Efficacy of Herbal Mono-drug Extracts and Their Combinations. Nat Prod Commun. 2009;4(2):1934578X0900400228. https://doi.org/10.1177/1934578X0900400228
12. Sholapuri P, Chintha V, Matcha B, Pradeepkiran J. Beneficial effects of polyherbal formulation (Bronco-T) on formaldehyde-induced lung toxicity in male Wistar rats. Toxicol Res (Camb). 2020;9(6):798–807. https://doi.org/10.1093/toxres/tfaa083
13. Johri RK, Zutshi U. An Ayurvedic formulation 'Trikatu' and its constituents. J Ethnopharmacol. 1992;37(2):85–91. https://doi.org/10.1016/0378-8741(92)90067-2
14. Peterson CT, Denniston K, Chopra D. Therapeutic Uses of Triphala in Ayurvedic Medicine. J Altern Complement Med. 2017;23(8):607–14. https://doi.org/10.1089/acm.2017.0083
15. Prasad S, Tyagi AK. Ginger and Its Constituents: Role in Prevention and Treatment of Gastrointestinal Cancer. Gastroenterol Res Pract. 2015;2015(1):142979. https://doi.org/10.1155/2015/142979
16. Stojanović-Radić Z, Pejčić M, Dimitrijević M, Aleksić A, V. Anil Kumar N, Salehi B, et al. Piperine-A Major Principle of Black Pepper: A Review of Its Bioactivity and Studies. Appl Sci. 2019;9(20):4270. https://doi.org/10.3390/app9204270
17. Sandhya T, Lathika KM, Pandey BN, Mishra KP. Potential of traditional ayurvedic formulation, Triphala, as a novel anticancer drug. Cancer Lett. 2006;231(2):206–14. https://doi.org/10.1016/j.canlet.2005.01.035
18. Mani K, Aiyalu R, Thiruvengadarajan VS, Arivukkarasu R, Suriyapriya K. A Comprehensive Review of Drynaria quercifolia (L.) J. Sm. Pharmacognosy Reviews. 2023 Jul 1;17(34).
19. Bose Mazumdar Ghosh A, Banerjee A, Chattopadhyay S. An insight into the potent medicinal plant Phyllanthus amarus Schum. and Thonn. Nucleus. 2022;65(3):437–72. https://doi.org/10.1007/s13237-022-00409-z
20. Timalsina D, Devkota HP. Eclipta prostrata (L.) L. (Asteraceae): Ethnomedicinal Uses, Chemical Constituents, and Biological Activities. Biomolecules. 2021;11(11):1738. https://doi.org/10.3390/biom11111738
21. Kaushik R, Jain J, Danish Khan A, Rai P. Trikatu - A combination of three bioavailability enhancers. Int J Green Pharm. 2018;12(3):S437–41.
22. Feng L, Zhai YY, Xu J, Yao WF, Cao YD, Cheng FF, et al. A review on traditional uses, phytochemistry and pharmacology of Eclipta prostrata (L.) L. J Ethnopharmacol. 2019;245:112109. https://doi.org/10.1016/j.jep.2019.112109
23. Sadeghi-Nejad B, Deokule SS. Anti-dermatophytic activity of Drynaria quercifolia (L.) J. Smith. Jundishapur J Microbiol. 2009;2(1):25–30.
24. Chaity FR, Khatun M, Rahman MS. In vitro membrane stabilizing, thrombolytic and antioxidant potentials of Drynaria quercifolia L., a remedial plant of the Garo tribal people of Bangladesh. BMC Complement Altern Med. 2016;16(1):184. https://doi.org/10.1186/s12906-016-1170-5
25. Khan A, Haque E, Mukhlesur Rahman M, Mosaddik A, Abdul Alim Al-Bari M, Rahman M. Antipyretic Activity of Rhizome of Drynaria quercifolia. in Rabbit. Pharm Biol. 2007;45(4):312–5. https://doi.org/10.1080/13880200701215075
26. Nisar MF, He J, Ahmed A, Yang Y, Li M, Wan C. Chemical Components and Biological Activities of the Genus Phyllanthus: A Review of the Recent Literature.

Molecules. 2018;23(10):2567. https://doi.org/10.3390/molecules23102567
27. Baliga MS, Meera S, Mathai B, Rai MP, Pawar V, Palatty PL. Scientific validation of the ethnomedicinal properties of the Ayurvedic drug Triphala: A review. Chin J Integr Med. 2012;18(12):946–54. https://doi.org/10.1007/s11655-012-1299-x
28. Lu K, Chakroborty D, Sarkar C, Lu T, Xie Z, Liu Z, et al. Triphala and Its Active Constituent Chebulinic Acid Are Natural Inhibitors of Vascular Endothelial Growth Factor-A Mediated Angiogenesis. PLoS One. 2012;7(8):e43934. https://doi.org/10.1371/journal.pone.0043934
29. Sudhanshu Kumar Jain, R. R. Rao. A Handbook of Field and Herbarium Methods. Scholarly Publications; 1977. 150 p.
30. Korrodi-Gregório L, Soto-Cerrato V, Vitorino R, Fardilha M, Pérez-Tomás R. From Proteomic Analysis to Potential Therapeutic Targets: Functional Profile of Two Lung Cancer Cell Lines, A549 and SW900, Widely Studied in Pre-Clinical Research. PLoS One. 2016;11(11):e0165973. https://doi.org/10.1371/journal.pone.0165973
31. Abubakar AR, Haque M. Preparation of Medicinal Plants: Basic Extraction and Fractionation Procedures for Experimental Purposes. J Pharm Bioallied Sci. 2020;12(1):1–10. https://doi.org/10.4103/jpbs.JPBS_175_19
32. Marles RJ, Farnsworth NR. Antidiabetic plants and their active constituents. Phytomedicine. 1995;2(2):137–89. https://doi.org/10.1016/S0944-7113(11)80059-0
33. Farnsworth NR. Biological and Phytochemical Screening of Plants. J Pharm Sci. 1966;55(3):225–76. https://doi.org/10.1002/jps.2600550302
34. Singleton VL, Orthofer R, Lamuela-Raventós RMBT-M in E. [14] Analysis of total phenols and other oxidation substrates and antioxidants by means of folin-ciocalteu reagent. In: Oxidants and Antioxidants Part A. Academic Press; 1999;299:152-78.
35. Zhishen J, Mengcheng T, Jianming W. The determination of flavonoid contents in mulberry and their scavenging effects on superoxide radicals. Food Chem. 1999;64(4):555–9. https://doi.org/10.1016/S0308-8146(98)00102-2
36. Prieto P, Pineda M, Aguilar M. Spectrophotometric Quantitation of Antioxidant Capacity through the Formation of a Phosphomolybdenum Complex: Specific Application to the Determination of Vitamin E. Anal Biochem. 1999;269(2):337–41. https://doi.org/10.1006/abio.1999.4019
37. Brand-Williams W, Cuvelier ME, Berset C. Use of a free radical method to evaluate antioxidant activity. LWT - Food Sci Technol. 1995;28(1):25–30. https://doi.org/10.1016/S0023-6438(95)80008-5
38. BLOIS MS. Antioxidant Determinations by the Use of a Stable Free Radical. Nature. 1958;181(4617):1199–200. https://doi.org/10.1038/1811199a0
39. Yesmin S, Paul A, Naz T, Rahman ABMA, Akhter SF, Wahed MII, et al. Membrane stabilization as a mechanism of the anti-inflammatory activity of ethanolic root extract of Choi (Piper chaba). Clin Phytoscience. 2020;6(1):59. https://doi.org/10.1186/s40816-020-00207-7
40. van Meerloo J, Kaspers GJ, Cloos J. Cell sensitivity assays: The mtt assay. Methods Mol Biol. 2011;731:237-45. https://doi.org/10.1007/978-1-61779-080-5_20.
41. Giard DJ, Aaronson SA, Todaro GJ, Arnstein P, Kersey JH, Dosik H, et al. In Vitro Cultivation of Human Tumors: Establishment of Cell Lines Derived From a Series of Solid Tumors2. J Natl Cancer Inst. 1973;51(5):1417–23. https://doi.org/10.1093/jnci/51.5.1417
42. Li T, Kon N, Jiang L, Tan M, Ludwig T, Zhao Y, et al. Tumor Suppression in the Absence of p53-Mediated Cell-Cycle Arrest, Apoptosis, and Senescence. Cell. 2012;149(6):1269–83. https://doi.org/10.1016/j.cell.2012.04.026
43. Ribble D, Goldstein NB, Norris DA, Shellman YG. A simple technique for quantifying apoptosis in 96-well plates. BMC Biotechnol. 2005;5(1):12. https://doi.org/10.1186/1472-6750-5-12
44. Trott O, Olson AJ. AutoDock Vina: Improving the speed and accuracy of docking with a new scoring function, efficient optimization, and multithreading. J Comput Chem. 2010;31(2):455–61. https://doi.org/10.1002/jcc.21334
45. Berman HM, Westbrook J, Feng Z, Gilliland G, Bhat TN, Weissig H, et al. The Protein Data Bank. Nucleic Acids Res. 2000;28(1):235–42. https://doi.org/10.1093/nar/28.1.235
46. Kim S, Thiessen PA, Bolton EE, Chen J, Fu G, Gindulyte A, et al. PubChem Substance and Compound databases. Nucleic Acids Res. 2016;44(D1):D1202–13. https://doi.org/10.1093/nar/gkv951
47. Schrödinger. PyMOL, molecular visualization system. Available from: https://pymol.org. 2018
48. Abraham MJ, Murtola T, Schulz R, Páll S, Smith JC, Hess B, et al. GROMACS: High performance molecular simulations through multi-level parallelism from laptops to supercomputers. SoftwareX. 2015;1–2:19–25. https://doi.org/10.1016/j.softx.2015.06.001
49. Jorgensen WL, Chandrasekhar J, Madura JD, Impey RW, Klein ML. Comparison of simple potential functions for simulating liquid water. J Chem Phys. 1983;79(2):926–35. https://doi.org/10.1063/1.445869
50. Kumari R, Kumar R, Lynn A. g_mmpbsa—A GROMACS Tool for High-Throughput MM-PBSA Calculations. J Chem Inf Model. 2014;54(7):1951–62. https://doi.org/10.1021/ci500020m
51. Benayad S, Wahnou H, El Kebbaj R, Liagre B, Sol V, Oudghiri M, et al. The Promise of Piperine in Cancer Chemoprevention. Cancers (Basel). 2023;15(22):5488. https://doi.org/10.3390/cancers15225488
52. Tungmunnithum D, Thongboonyou A, Pholboon A, Yangsabai A. Flavonoids and Other Phenolic Compounds from Medicinal Plants for Pharmaceutical and Medical Aspects: An Overview. Medicines. 2018;5(3):93. https://doi.org/10.3390/medicines5030093
53. Kandhavelu J, Subramanian K, Naidoo V, Sebastianelli G, Doan P, Konda Mani S, et al. A novel EGFR inhibitor, HNPMI, regulates apoptosis and oncogenesis by modulating BCL-2/BAX and p53 in colon cancer. Br J Pharmacol. 2024;181(1):107–24. https://doi.org/10.1111/bph.16141